A PREDICTIVE MODEL FOR TACTILE FORCE ESTIMATION USING AUDIO-TACTILE DATA

ABSTRACT

Robust in-hand manipulation of objects with movable content requires estimation and prediction of the contents' motion with enough anticipation to allow time to compensate for resulting internal torques. The quick estimation of the objects' dynamics can be challenging when the objects' motion properties (e.g., type, amount, dynamics) cannot be observed visually due to robot occlusions or opacity of the container. This can be further complicated by the computational requirements of onboard hardware available for real-time processing and control for robotics. In this work, we develop a simple learning framework that uses echo state networks to predict the torques experienced on the robotic hand with enough anticipation to allow for adaptive controls and sufficient efficiency for real-time prediction without GPU processing. We demonstrate the efficacy of this formulation for tactile force prediction on the Allegro robotic hand with a Tekscan tactile skin using both material-specific and material-agnostic learned models. We show that while both are effective, the material-specific models show an improvement in accuracy due to the difference in inertial properties between the different materials. We also develop a prediction model that uses audio feedback to augment the tactile predictions. We show that adding auditory feedback improves the prediction error, though it significantly increases the computation cost of the model. We validate this formulation for online prediction on the robotic hand moving materials in real-time and adapting grip for slip detection.

1 INTRODUCTION

Safe in-hand manipulation of objects requires the ability to the estimate and adapt to the forces experienced by the robot hand from the objects' inertial forces during motion.

Our contributions to this study are twofold. First, we establish the feasibility of blending autoregressive text-to-image models with LLMs into a unified architecture that retains the core strengths of each while revealing new, emergent capabilities. Second, we present innovative strategies for multimodal instruction tuning, utilizing text-based instructions and a custom-curated dataset designed explicitly for image generation. The result is a first-of-its-kind large multimodal model which can coherently generate long-form content with interleaved text and images.

2 RELATED WORK

Tactile estimation and prediction research has been of great interest in manipulation applications. Much of the research focuses on slip detection and reactive adaptation, discussed in detail in [1], [2]. Some methods use neural networks for slip detection using tactile data or vision-based tactile sensors for classifying contact or slippage [3]–[7]. Tactile and audio data are sometimes used in neural networks for content estimation, such as weight estimation or liquid height [8], [9]. Other methods learn models of liquid flow of unknown materials by using tactile or force data to estimate physical properties of the contents, including mass, volume and viscosity [10], [11]. These models are used to classify unknown liquids and for content estimation, which could be used to predict flow over time for manipulation. Here, we investigate the use of low-dimensional model learning for general content estimation, without imposing the structure of physical models of liquid flow that the learning here relies upon. Other research uses tactile force estimation and prediction for control and manipulation, discussed in depth in [12]. Many methods use estimation of contact point, force

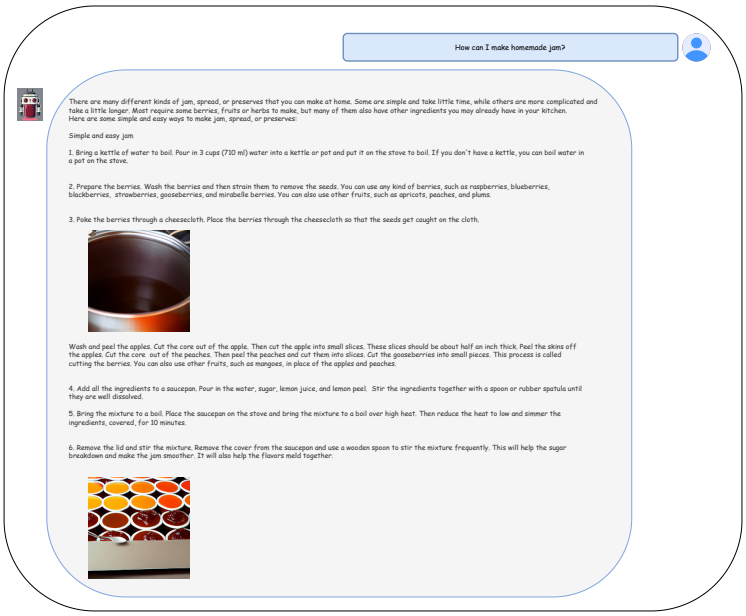

Figure 1: Selected sample generated by our instruction-tuned JAM-Cross model. The model can complex mixed-modal outputs with coherent alignment between generated text and images.

and curvature to drive control for manipulation [6], [13], [14]. Other research methods use neural networks to learn contact force estimation from tactile data [7], [15]. Su et al. [7] uses a neural network to predict the contact forces in the fingertips. The contact force estimation focuses on static grasping (i.e. when the container contents are not moving) to enable slip detection and slip prevention during grasping. [16] also performs force estimation for Biotac sensors located in the fingertips. They use convolutional neural networks to estimate forces during contact, which could be used in a grasp controller. [17] and [18] use graph neural networks and convolutional LSTMs respectively to predict contact forces in the fingertips during grasping. Both use the prediction models to assess grasp stability during lifting. Other methods use deep learning or reinforcement learning to drive touch-based manipulation through unsupervised learning [19], [20]. These methods require large amounts of data (3000-5000 trajectories) and prediction is done on short time horizons (15-18 time steps) due to the complexity of the prediction model. The approach proposed in this paper however focuses developing prediction models that have faster training times and lower complexity for longer time horizon predictions (up to 3 seconds into the future) to accommodate reactive controllers that require grasp adaptation. Echo state networks [21], [22] are a type of recurrent neural network with a random dynamical resevoir (i.e., randomly connected neurons within the reservoir). These networks have been shown to be faster to train, requiring fewer parameters to be optimized and not suffering from gradient issues found in methods that use gradient-based optimization (i.e., backpropogation). [23] uses echo state networks to predict the tactile signature of an antenna from action. They use the ESN for the 1-dimensional tactile prediction to discriminate when contact is occurring, rather than for grip control. Furthermore, their work uses echo state networks to predict one time step into the future, rather than for a longer time horizon (e.g., 300 steps into the future) as performed in this work. Furthermore, the other work only use tactile sensors for prediction and estimation. Here, we use auditory feedback to augment the tactile prediction. While there has been research in using auditory feedback for tactile applications [24]–[27], most work focuses on using the multimodal perception for classification and object property identification, rather than real-time tactile prediction.

2.1 Continued Pretraining

We combine the two pretrained models into a singular, cohesive structure in our proposed framework. This composite model is fine-tuned using a hybrid dataset comprising both text-only and image-text samples within our *continued pretraining* phase. The central motivation behind this approach is to

seamlessly merge the capabilities of two pretrained models, capitalizing on the unique strengths of each.

3 METHODS

We develop a framework for learning and predicting the tactile pressure distribution experienced in a robotic hand. Specifically, we use echo state networks (ESNs) [21] to learn a predictive model of the magnitude and center of pressure on the hand caused by the objects' movement during manipulation. We describe below the experimental setup and the formulation for the model learning and tactile force prediction.

3.1 CONTINUED PRETRAINING

We combine the two pretrained models into a singular, cohesive structure in our proposed framework. This composite model is fine-tuned using a hybrid dataset comprising both text-only and image-text samples within our *continued pretraining* phase. The central motivation behind this approach is to seamlessly merge the capabilities of two pretrained models, capitalizing on the unique strengths of each.

3.1.1 MODEL MERGING

The concept of model merging has been previously utilized to combine models that share identical optimization trajectories (Kaddour et al., 2022), or models that are trained on identical datasets but have independent optimizations (for instance, Matena & Raffel (2022); Wortsman et al. (2022); Ainsworth et al. (2022)). A consistent approach across these studies is to combine models without any training. Our approach diverges from this convention; we view the merged model as a powerful initialization for subsequent training on mixed-modal data. The weights of the averaged model are defined as:

$$\boldsymbol{\theta}_{average} = \frac{1}{2}\boldsymbol{\theta}_{llm} + \frac{1}{2}\boldsymbol{\theta}_{img} \tag{1}$$

Where $\boldsymbol{\theta}_{llm}$ and $\boldsymbol{\theta}_{img}$ represent the weights of the LLM and the text-to-image model respectively. In this study, we explore weights merging specifically to multimodal decoder-only large transformer models, and notably, on an unprecedented scale, involving models trained on trillions of tokens from diverse datasets. In the following sections, we refer to our average model as JAM-Uniform.

3.1.2 WIDTH CONCATENATION

Our second approach employs the pretrained weights to initialize a wider architecture. Our new model has hidden dimensions $d_{joint} = 8192$, which is doubled with respect to one of the two original models $d_{llm} = d_{img} = 4096$. We keep the same number of layers of the original architectures. The resulting architecture has 26B parameters, initialized starting from the pretrained weights of our backbones. The token embedding input/output projections and the learned positional embeddings of the two initial models are concatenated on the hidden dimension. The attention weights (e.g query projection) $\boldsymbol{W}_{q,combined} \in \mathbb{R}^{d_{joint} \times d_{joint}}$ are initialized as:

$$\boldsymbol{W}_{q,combined} = \begin{pmatrix} \boldsymbol{W}_{q,llm} & \boldsymbol{W}_{q,llm} \\ \boldsymbol{W}_{q,img} & \boldsymbol{W}_{q,img} \end{pmatrix} \tag{2}$$

Where $\boldsymbol{W}_{q,llm}, \boldsymbol{W}_{q,img} \in \mathbb{R}^{d_{llm} \times d_{llm}}$ represent the weights for the query projection of a generic attention layer. All the other weights (FFNs and output projections) are initialized following the same logic. We also experiment with slight variations of the approach:

$$\boldsymbol{W}_{q,combined} = \begin{pmatrix} \boldsymbol{W}_{q,llm} & \boldsymbol{W}_{q,average} \\ \boldsymbol{W}_{q,img} & \boldsymbol{W}_{q,average} \end{pmatrix} \tag{3}$$

Instead of copying the two models' parameters, we use the average to initialize half of the new parameters. We name the resulting model JAM-Width.

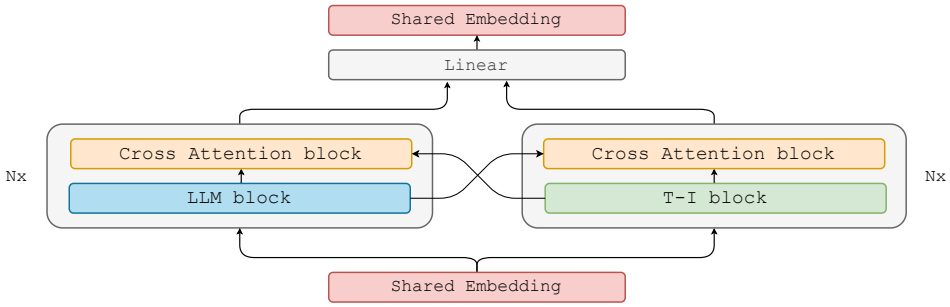

Figure 2: JAM-Cross, architecture overview. The cross-attention blocks are interleaved between the original LLM block and the Text-Image blocks, and the output embedding between the two branches are concatenated and then projected to the output embedding dimension.

3.1.3 Cross Model Fusion

We propose to embed cross-attention layers between the foundational models to facilitate seamless information interchange while preserving the original models' knowledge. Given two decoder-only transformers models $\mathcal{T}_{llm}$ and $\mathcal{T}_{img}$, we introduce a bi-directional cross-attention mechanism that enables the layers of one model to attend to the corresponding layer's output of the other model. This approach allows for a progressive exchange of information at different representation levels. For a specific layer l, let the models produce sequences of hidden states $\boldsymbol{H}_{llm,l}$ for $\mathcal{T}_{llm}$ and $\boldsymbol{H}_{img,l}$ for $\mathcal{T}_{llm}$ where these hidden states are outputs from layer l. The output of the cross-attention mechanism ($\boldsymbol{H}_{cross,l}$) from $\mathcal{T}_{img} \rightarrow \mathcal{T}_{llm}$ for a given layer is evaluated as:

$$\boldsymbol{Q}_{cross,l} = \boldsymbol{W}_{q,l}\boldsymbol{H}_{llm,l-1}, \quad \boldsymbol{K}_{cross,l} = \boldsymbol{W}_{k,l}\boldsymbol{H}_{img,l-1}, \quad \boldsymbol{V}_{cross,l} = \boldsymbol{W}_{v,l}\boldsymbol{H}_{img,l-1} \tag{4}$$

$$\boldsymbol{H}_{cross,l} = \text{Softmax}\left(\frac{\boldsymbol{Q}_{cross,l}\boldsymbol{K}^T_{cross,l}}{\sqrt{d_k}}\right) \tag{5}$$

Where W_q, W_k, W_v represent the query, key, and value projection weights of the newly inserted cross-attention layers. A symmetric process is applied for the reverse direction $\mathcal{T}_{llm} \rightarrow \mathcal{T}_{img}$. We use a shared input-output projection layer, initializing the weights of the text tokens from the LLM input embedding and the weights of the image tokens from the image-text model. We insert a new linear projection layer that takes the concatenation of the two model's output embeddings as input. Figure 2 illustrates a schematic of our model configuration. We refer to the model resulting from this approach as JAM-Cross. Additional architectural details and the underlying design choices can be found in Sect. 4.1. The ablation study for the optimal frequency of inserting new layers is presented in Sect. 4.3.

3.2 Multimodal Conversational Instruct Tuning

Supervised fine-tuning is a fundamental tool to leverage the abilities of large pretrained models. Recently, instruct tuning has been extended to a multimodal setting (Liu et al., 2023; Dai et al., 2023); however, all the existing approaches are focused on visual understanding abilities. In this work, we study instruction tuning tailored to interleaved image-text generation. We collect a small and curated mixed-modal dataset to teach our JAM model to support textual explanations with coherent images. Since in the first stage, the model has been trained on image-text captions and text-only data; we train on interleaved image-text data during this phase. In line with the superficial alignment hypothesis introduced in LIMA (Zhou et al., 2023), we demonstrate that the model can quickly learn the style of images and text from a small curated dataset. Our results suggest that the Superficial Alignment Hypothesis introduced in LIMA holds not only for learning the text style but also for images. In our experiments, we consider two slightly different instruction tuning settings, we introduce a small portion of the image-text Shutterstock data with retrieval augmentation and we find this approach beneficial to preserve the generated image quality when generating with retrieval augmentation. Sect 4 presents a comparison between these two strategies. We train using a standard supervised procedure without leveraging any reinforcement learning or human preference strategy. In this instruction-tuning

phase, we leverage interleaved image-text data in contrast to previous methods (Koh et al., 2023a) that rely only on image-text caption and no instruction tuning, our experimental results confirm the benefits of training with interleaved image-text data.

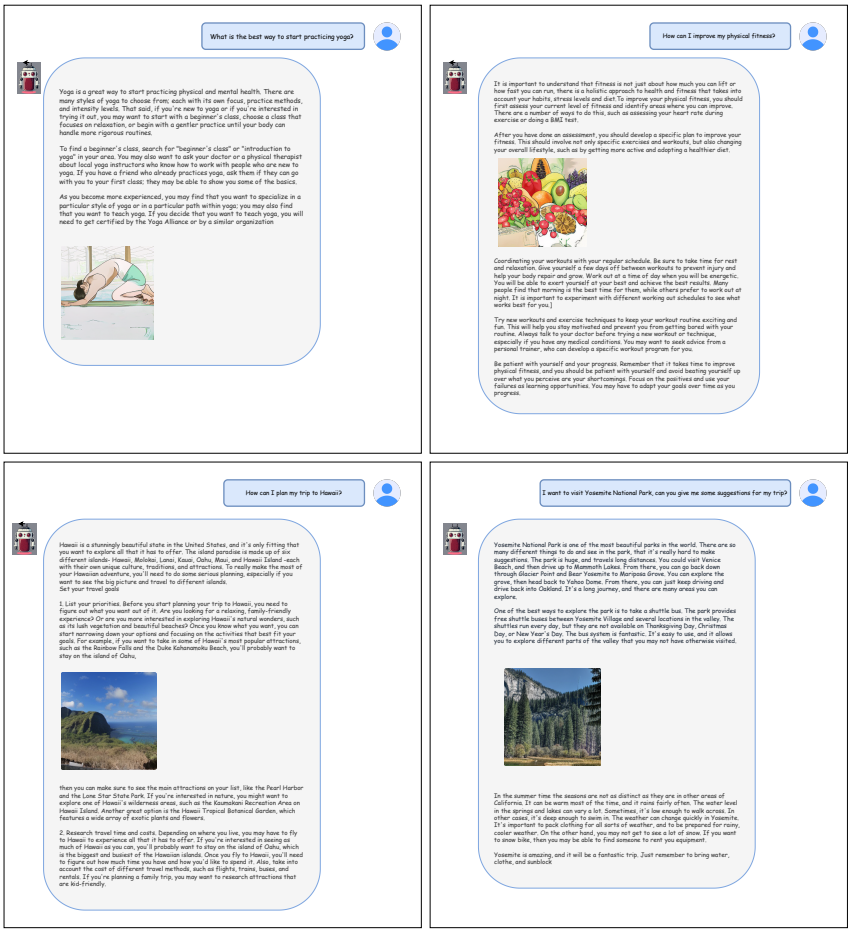

Figure 3: Selected samples generated by our JAM-Cross instruct tuned model. (Top - generated without retrieval augmentation; Bottom - generated with retrieval augmentation)

4 EXPERIMENTS

4.1 EXPERIMENTAL DETAILS

Tokenizers For images, we use the VQ-VAE tokenizer from Gafni et al. (2022). The image resolution is set to 256×256, 1024 tokens represent each image, and the vocabulary has a size of 8192. Our text tokenizer is the same that have been used to train the two parent models, trained over the Zhang et al. (2022) data for text. We introduce the additional <break> token used by CM3leon to identify a modality break.

Image-Text Autoregressive Model We adopt CM3leon as the image-text autoregressive backbone. The model has a standard decoder-only architecture with some peculiarities: no bias terms, dropout, and learnable parameters for layer norms. It has been trained on 2.4T image-text tokens and uses a sequence length 4096.

LLM As an LLM backbone, we select a model with the same architecture as CM3leon, trained in Molybog et al. (2023) this allows us to experiment with a broader range of approaches, such as

weight averaging and width concatenation. The model is trained on 1.4T text data with a 2048 context length, and we further fine-tuned it with a 4096 context length using only 30B text tokens.

Objective In all our experiments, we employ the CM3 objective introduced in Aghajanyan et al. (2022); this objective accepts the original sequence as input or transforms it into an infilling instance by masking specific spans and relocating them to the end. Then, the model is optimized for minimizing the standard autoregressive loss $-\log p(x_{input})$. This objective allows for optional bidirectionally and increases the versatility of the model that can be used for both infilling or standard autoregressive generation. We prevent the objective from masking across the modality <break> tokens.

Retrieval Augmentation We employ multimodal retrieval augmentation introduced in Yasunaga et al. (2022) for our training procedure. We leverage our text-to-image backbone's modifications introduced in Yu et al. (2023). The retrieval procedure employs a dense retriever and a specifically selected retrieval strategy. The retriever takes an input query x and returns a relevance score $r(q, m)$ for each candidate document m in our memory bank $\mathcal{M}$. Each multimodal document is split between text and images and fed to the corresponding modality-specific VIT-B-32 CLIP encoder (Radford et al., 2021). The two embeddings are then averaged to form the documents' vector representation. We then use Maximum Inner Product Search (MIPS) over the memory bank to obtain a list of candidates. When sampling retrieved documents, we prioritize the diversity of the sampled documents by skipping candidates with a score $r(q, m) \leq 0.9$. Query dropout is applied to regularize the training, dropping 20% of tokens from the input sequence x.

Training - Alignment Phase During the continued pretraining, we train for approximately 50B multimodal tokens. Our initial learning rate is $lr = 3 \times 10^{-5}$ we use 500 warm-up steps. We set our optimal batch size to 8M tokens, this hyperparameter is borrowed from the mixed-modal scaling laws introduced in Aghajanyan et al. (2023). The total number of training steps is 5960. This training procedure takes approximately one day on 256 80GB A100s for all models. We select the last checkpoint for all the different JAM models, which is always the one with the lowest average validation PPL. All our training procedures are implemented using Metaseq[1].

Training - Instruct Tuning Our instruct tuning training procedure is data efficient we train with our instruction tuning mixed corpora. The initial learning rate is set to 1×10^{-5}, and we use 300 warm-up steps and a batch size of 1M. The instruction tuning procedure takes less than 2 hours on 64 80GB A100s, we train for 15 epochs over our mixture of datasets and manually select the best checkpoint corresponding to the 9th epoch. Following Zhou et al. (2023), we notice that the validation PPL doesn't correlate with the quality of the responses.

Decoding Strategies We implement a mixed-modal decoding strategy for our interleaved generation. The model starts generating text tokens until a modality <break> token is detected, then an image is sampled, and the generation continues until a <eos> token is sampled. We employ temperature sampling, a common technique used in autoregressive model (e.g Ramesh et al. (2022)) to control the randomness of the prediction by modifying the softmax temperature τ. We pair this technique with TopP sampling introduced in Holtzman et al. (2019) consisting of sampling from the top-ranked tokens with a cumulative probability exceeding a predefined threshold τ_P. We also employ classifier-free guidance (CFG (Gafni et al., 2022)) for sampling images. This technique allows to condition the sampling procedure, blending the logits from an unconditional sample with the logits from a conditional sample. The procedure is mathematically described as

$$\text{logits}_{cf} = \text{logits}_{uncond} + \alpha_c(\text{logits}_{cond} - \text{logits}_{uncond}) \tag{6}$$

where $\text{logits}_{cond} = \mathcal{T}(t_y|t_x)$ and $\text{logits}_{uncond} = \mathcal{T}(t_y| < mask >)$; $\mathcal{T}$ represent the transformer model, $< mask >$ represent the absence of the input text, t_x are the conditional input tokens, t_y are the output tokens and α_c is the scaling factor for CFG. Thanks to the CM3 objective, our training procedure allows our models to sample with CFG without further fine-tuning. Inspired by Yu et al. (2023) we complement this technique to boost the generation quality. Our samples are generated using a temperature value $\tau = 1$, τ_P is set between 0.8 and 1, and we use classifier-free guidance with values 3.5 and 4. In contrast to other approaches, we don't make use of the computationally

[1]https://github.com/facebookresearch/metaseq

Table 1: Zero Shot Text Comparison on Common Sense Reasoning Tasks

Model	Size	PIQA	ARC-C	ARC-E	StoryCloze	Winograd	Winogrande
GPT-3	175B	81.0	51.4	68.8	-	-	70.1
LLaMa	7B	79.8	47.6	72.8	-	-	70.1
LLM-4k	7B	76.7	45.9	67.7	79.3	83.9	66.2
JAM-Uniform	7B	62.4	28.5	42.6	63.5	47.8	49.7
JAM-Width	26B	57.8	31.4	31.6	54.7	50.2	51.9
JAM-Cross	19B	75.4	41.6	67.2	79.8	81.0	66.0

expensive clip-reranking (Ramesh et al., 2021; Yu et al., 2022; Gafni et al., 2022) or constrastive decoding (Li et al., 2022; Yu et al., 2023).

4.1.1 DATASETS

Shutterstock We randomly sample a subset of 30B tokens from CM3leon (Yu et al., 2023) pretraining data. The data consists of legally acquired image-caption pairs from Shutterstock, a commercial online platform offering images with ownership attribution and clear licensing terms.

Text corpora We use 30B text tokens sampled from a mixture of several publicly available data, and we reuse the data used for training other common open-source LLM following the same preprocessing of (Touvron et al., 2023). The datasets are: English CommonCrawl (Touvron et al., 2023), C4 (Raffel et al., 2020), Wikipedia, Books3 from ThePile (Gao et al., 2020), and arXiv.

LIMA We use the 1k dataset present in Zhou et al. (2023), which features various curated prompts and responses.

wikiHow We collect an interleaved image-text dataset sampling 3000 articles from WikiHow, an online wiki publication that usually curates apposite images for each article. We sample balanced articles from each category to ensure diversity; moreover, we leverage the platform's community ratings to filter each article's quality, sampling only those with a score greater than $90/100$. For each article, we use the title (e.g., *'How to make ..?'*) as prompt, we modify the phrase *'This article...'* with *'The following answer..'*. Furthermore, we restrict the number of images as 3 per sample, to fit our 4096 context length.

4.2 CONTINUED PRETRAINING RESULTS

In the initial stage of continued pretraining, we evaluate the performance across various JAM models. Our primary objective is to ensure minimal performance degradation post-merging, relative to the parent models. Managing both image and text processing within a single model poses significant challenges. This evaluation seeks to quantify the retention of original performance in our different JAM models, benchmarked against the two parent models specialized in individual modalities.

4.2.1 TEXT MODALITY

For the text modality, we compare the zero-shot performance on some common sense reasoning tasks: PIQA (Bisk et al., 2020), ARC-Challenge, ARC-Easy (Clark et al., 2018), StoryCloze (Mostafazadeh et al., 2016), Winograd, and Winogrande (Sakaguchi et al., 2021). We also report some recent influential LLM (Brown et al., 2020; Touvron et al., 2023), and our LLM (Molybog et al., 2023) fine-tuned with 4k context as a reference. Results are presented in Table 1. The JAM-Uniform reaches slightly better text-only performance than JAM-Width however, it is crucial to remark that this approach consolidates the functionalities of both parent models within a constrained 7B parameter space. Our findings reveal that the intrinsic knowledge of the parent models can be recovered mainly from the parameter average utilizing only a minimal portion of the original pretraining data. The JAM-Cross model yields the best results, aligning with our primary LLM. This highlights the strength of our bidirectional cross-attention mechanism against other baselines.

Table 2: Image-Text Comparison

Model	Size	MS-COCO PPL
CM3	2.7B	200.1
RA-CM3	2.7B	193.1
CM3leon	760M	168.8
CM3leon	7B	149.0
JAM-Uniform	7B	177.5
JAM-Width	26B	159.5
JAM-Cross	19B	**147.6**

Table 3: Ablations - JAM-Width Model

Init.	Wikipedia PPL	MS-COCO PPL
Copy	**7.34**	**159.5**
Average	9.0	175.4

Table 4: Ablations - JAM-Cross Model

C-Attn	Size	Wikipedia PPL	MS-COCO PPL
✗	13B	7.86	153.2
1	26B	7.53	152.4
2	19B	**7.18**	**149.0**
4	16B	8.55	151.7

Table 5: Ablations - Instruction Tuning

Shutterstock	MS-COCO PPL
✗	190.2
✓	164.5

4.2.2 IMAGE-TEXT MODALITY

To assess the performance of our different baselines over the image-text modality, we compare them using the validation PPL on MS-COCO dataset (Lin et al., 2014). We believe this metric robustly correlates with performance on subsequent tasks, such as image generation and captioning. Furthermore, it provides a reliable reference point for comparing different autoregressive models sharing an identical tokenizer. Results are reported in Table 2. Diverging from results on the text-only modality, the JAM-Width model exhibits enhanced performance over the JAM-Uniform model in the image-text domain. Specifically, the JAM-Width model demonstrates superior efficacy in retaining image-text performance relative to text-only performance. Conversely, despite a decline in performance, the JAM-Uniform model remains a good parameters-performance trade-off. Interestingly, our JAM-Cross model not only reaches the best PPL between the JAM strategies but also surpasses our foundational image-text model, CM3leon. We hypothesize that such advancement can be attributed to integrating novel textual capabilities coupled with an augmented parameter count inherent to the combined architecture. Based on empirical evidence, the JAM-Cross emerges as the best strategy to combine two pretrained autoregressive models.

4.2.3 INTERLEAVED GENERATION

Our instruct-tuned JAM-Cross model reaches a high-quality level of image-text generated output. To demonstrate its ability to generate coherent modality interleaved responses, we show an extensive set of generated samples in Figure 3 and Section **??**. The samples generated with retrieval are obtained from the model instruct-tuned with a mixture of pretraining image-text Shutterstock data along with our corpora of instruct-tuning datasets, while the samples generated without retrieval are obtained from the model instruct tuned only on our instruct-tuning set. The generated samples show coherent image and text integration, demonstrating unprecedented abilities at this novel task. Overall we find our retrieval augmented solution to be more effective than standard image sampling, boosting image quality. We further report several qualitative comparisons with the most relevant previous work GILL (Koh et al., 2023a) that features mixed-modal generation. We use our retrieval-augmented JAM-Cross model and source generations for the GILL model from the original paper. From this comparison (Figure 4), it's immediate to notice how our model has a better overall quality of responses. The generated text is more complete and exhaustive, while the generated images are more relevant to the text context. We remark that our method is the first capable of such coherent and interleaved generation with a focus on instruction tuning and that our fine-tuning procedure is effective in efficiently learning the style of the dataset, not only for text but even for images. Our model paves the way toward a larger adaption of mixed-modal generation in real-world use cases.

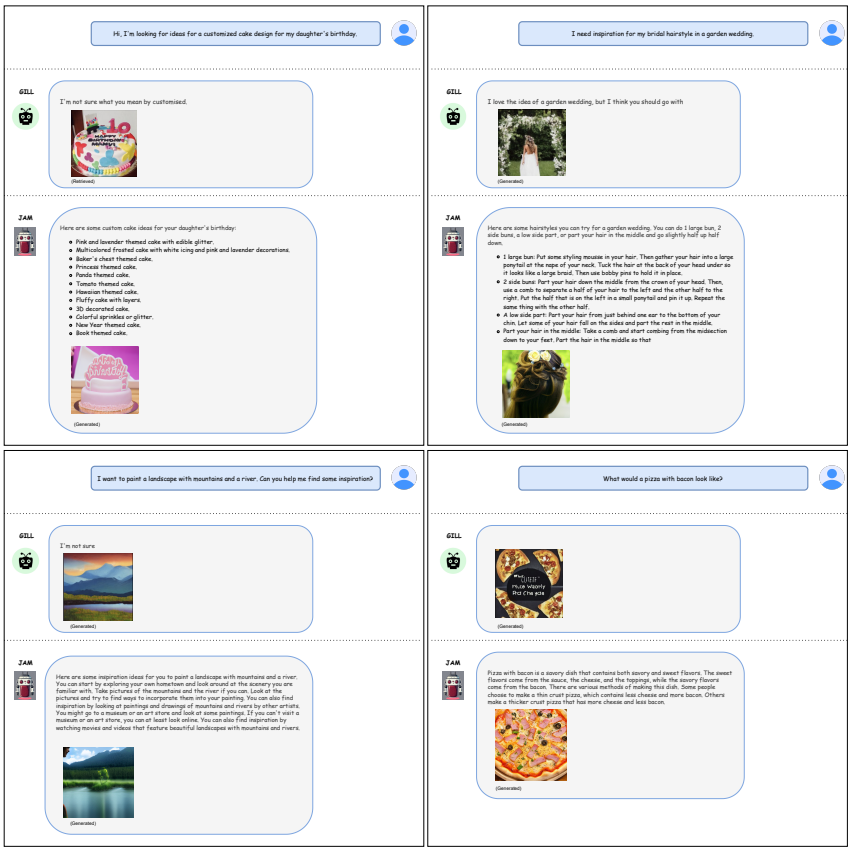

Figure 4: Qualitative comparison with previous interleaved generation models. Compared to GILL, our model is able to generate more complete and precise answers. Results for GILL are sourced from Koh et al. (2023a).

4.3 Ablation Study

We compare the two approaches for the width concatenation model: copying the original models' weight or using the average to initialize the new parameters. Results (Table 3) show that copying the weights is more effective than averaging them to retain the original model capabilities. The ablation study for the Cross-attention model is presented in Table 4. We ablate the frequency of inserting cross-attention layers and the impact of not using any cross-attention layers. These experiments are performed training with 25B tokens, all the other parameters are the same as reported in Sect. 4.1. We remark that this is an even shorter training setting concerning our 50B tokens total training and that the difference in performance increases as the training progresses. We further ablate the contribution of image-text pretraining data in the instruction tuning procedure in Table 5. The results indicate the importance of using pretraining data mixed in the instruction tuning procedure to preserve the MS-COCO PPL. We do not report WikiHow PPL since analyzing the models shows that it doesn't correlate with generation quality similarly to Zhou et al. (2023).

5 Related Works

Generative Text-to-Image Models The field of generative text-to-image models has recently been dominated by diffusion models (Sohl-Dickstein et al., 2015; Ho et al., 2020). Recent enhancements have used pretrained text representations (Ramesh et al., 2022; Nichol et al., 2022) like CLIP (Radford et al., 2021) to improve the generation quality. Concurrently to developing diffusion-based generative models, significant steps have been made by autoregressive token models (Esser et al., 2021; Gafni et al., 2022). These models encode images into a discrete latent space (Van Den Oord et al., 2017) and can be processed as a standard sequence-to-sequence modeling task, enabling the borrowing

of techniques used from Large Language Models. A critical element that has been found beneficial in boosting text-to-image generative models is retrieval augmentation (Chen et al., 2022; Yasunaga et al., 2022). Yasunaga et al. (2022) propose to prefix decoder-only models, such as Aghajanyan et al. (2022), with retrieved images during training, resulting in a huge efficiency gain for the training procedure. Yu et al. (2023), scale this strategy to reach state-of-art performance in image generation using 5x less training compute. In this work, we borrow their model as our text-to-image autoregressive backbone.

Multimodal Language Models The multimodal language model field has recently seen considerable development. Several prior works have focused on connecting language models to visual encoders. (Tsimpoukelli et al., 2021; Mokady et al., 2021; Najdenkoska et al., 2023; Li et al., 2023). These methods typically train a mapping network between a pretrained image encoder and a language model. Flamingo (Alayrac et al., 2022) introduces cross attention into a frozen LLM to inject visual features and trains a large corpus of image-text pairs. In this work, we similarly use cross attention to bridge the two models; however, our mechanism is bidirectional between the vision and language models, while for Flamingo, the visual knowledge is injected in the language model and not vice-versa. CM3 (Aghajanyan et al., 2022) is trained on a large corpus of structured HTML; it introduces the Casually Masked Language Modeling objective we adopt to train our models. Koh et al. (2023b) propose a multimodal language model capable of processing arbitrarily interleaved image and text inputs and generating interleaved output of text and retrieved image. Subsequently, on the same line of work, GILL Koh et al. (2023a) proposes to ground an LLM to a text-to-image model, using a mapping network and freezing the pretrained models, introducing the possibility of generating or retrieving images as output.

Instruction Tuning Instruction tuning aims to teach language models to follow natural language instructions. Several methods have been proposed for instruction tuning, using existing NLP datasets converted in instruction formats Wei et al. (2021) Chung et al. (2022), or using LLMs like GPT-4 to generate instruction data with better diversity Wang et al. (2022) Honovich et al. (2022). Recently, LIMA Zhou et al. (2023) demonstrated that 1,000 carefully curated samples are enough to reach competitive results compared to bigger instruction-tuning datasets. The authors hypothesize that most of the knowledge is learned during the pretraining, and the instruction tuning teaches the style to interact with the users. In this work, we explore using a small set of multimodal instruction tuning data to fine-tune our model, verifying the effectiveness of a small dataset in this multimodal setting tailored to image generation. Several vision language works adopt instruction tuning for multimodal tasks-focused user interactions optimized for visual content understanding Liu et al. (2023) Dai et al. (2023) Ye et al. (2023) Zhu et al. (2023). Unlike previous works, we explore instruction tuning focused mixed-modal generation, paving the way for more significant adaptation of multimodal models that can generate interleaved image-text output.

6 Conclusions

In this work, we have presented novel methodologies for combining pretrained autoregressive models, demonstrating the viability of synthesizing the knowledge of two distinct models into a cohesive structure with extended capabilities. Our exploration validates that the integrated model can be adeptly fine-tuned using our tailored instruction-tuning procedure for interleaved image-text generation. To this end, we pioneered creating a specialized dataset centered on instruction tuning for this particular task. Nevertheless, the proposed study is limited to 7B parameter models with the same architecture. Future works may consider scaling the models' size and asymmetrically applying our cross-fusion method to bridge models of varying sizes. Increasing the context length and delving into multi-turn conversations could further represent an interesting exploration direction. In conclusion, our study sets the foundation for substantial advancements in the realm of multimodal autoregressive models. The fusion of text-to-image generation with large language models paves the way for sophisticated systems capable of interleaved image-text interactions, enriching the landscape of conversational AI.

References

Armen Aghajanyan, Bernie Huang, Candace Ross, Vladimir Karpukhin, Hu Xu, Naman Goyal, Dmytro Okhonko, Mandar Joshi, Gargi Ghosh, Mike Lewis, et al. Cm3: A causal masked

multimodal model of the internet. *arXiv preprint arXiv:2201.07520*, 2022.

Armen Aghajanyan, Lili Yu, Alexis Conneau, Wei-Ning Hsu, Karen Hambardzumyan, Susan Zhang, Stephen Roller, Naman Goyal, Omer Levy, and Luke Zettlemoyer. Scaling laws for generative mixed-modal language models. *arXiv preprint arXiv:2301.03728*, 2023.

Samuel Ainsworth, Jonathan Hayase, and Siddhartha Srinivasa. Git re-basin: Merging models modulo permutation symmetries. In *The Eleventh International Conference on Learning Representations*, 2022.

Jean-Baptiste Alayrac, Jeff Donahue, Pauline Luc, Antoine Miech, Iain Barr, Yana Hasson, Karel Lenc, Arthur Mensch, Katherine Millican, Malcolm Reynolds, et al. Flamingo: a visual language model for few-shot learning. *Advances in Neural Information Processing Systems*, 35:23716–23736, 2022.

Yonatan Bisk, Rowan Zellers, Jianfeng Gao, Yejin Choi, et al. Piqa: Reasoning about physical commonsense in natural language. In *Proceedings of the AAAI conference on artificial intelligence*, volume 34, pp. 7432–7439, 2020.

Tom Brown, Benjamin Mann, Nick Ryder, Melanie Subbiah, Jared D Kaplan, Prafulla Dhariwal, Arvind Neelakantan, Pranav Shyam, Girish Sastry, Amanda Askell, et al. Language models are few-shot learners. *Advances in neural information processing systems*, 33:1877–1901, 2020.

Wenhu Chen, Hexiang Hu, Chitwan Saharia, and William W Cohen. Re-imagen: Retrieval-augmented text-to-image generator. *arXiv preprint arXiv:2209.14491*, 2022.

Hyung Won Chung, Le Hou, Shayne Longpre, Barret Zoph, Yi Tay, William Fedus, Eric Li, Xuezhi Wang, Mostafa Dehghani, Siddhartha Brahma, et al. Scaling instruction-finetuned language models. *arXiv preprint arXiv:2210.11416*, 2022.

Peter Clark, Isaac Cowhey, Oren Etzioni, Tushar Khot, Ashish Sabharwal, Carissa Schoenick, and Oyvind Tafjord. Think you have solved question answering? try arc, the ai2 reasoning challenge. *arXiv preprint arXiv:1803.05457*, 2018.

Wenliang Dai, Junnan Li, Dongxu Li, Anthony Meng Huat Tiong, Junqi Zhao, Weisheng Wang, Boyang Li, Pascale Fung, and Steven Hoi. Instructblip: Towards general-purpose vision-language models with instruction tuning. *arXiv preprint arXiv:2305.06500*, 2023.

Patrick Esser, Robin Rombach, and Bjorn Ommer. Taming transformers for high-resolution image synthesis. In *Proceedings of the IEEE/CVF conference on computer vision and pattern recognition*, pp. 12873–12883, 2021.

Oran Gafni, Adam Polyak, Oron Ashual, Shelly Sheynin, Devi Parikh, and Yaniv Taigman. Make-a-scene: Scene-based text-to-image generation with human priors. In *European Conference on Computer Vision*, pp. 89–106. Springer, 2022.

Leo Gao, Stella Biderman, Sid Black, Laurence Golding, Travis Hoppe, Charles Foster, Jason Phang, Horace He, Anish Thite, Noa Nabeshima, et al. The pile: An 800gb dataset of diverse text for language modeling. *arXiv preprint arXiv:2101.00027*, 2020.

Jonathan Ho, Ajay Jain, and Pieter Abbeel. Denoising diffusion probabilistic models. *Advances in neural information processing systems*, 33:6840–6851, 2020.

Ari Holtzman, Jan Buys, Li Du, Maxwell Forbes, and Yejin Choi. The curious case of neural text degeneration. In *International Conference on Learning Representations*, 2019.

Or Honovich, Thomas Scialom, Omer Levy, and Timo Schick. Unnatural instructions: Tuning language models with (almost) no human labor. *arXiv preprint arXiv:2212.09689*, 2022.

Jean Kaddour, Linqing Liu, Ricardo Silva, and Matt J Kusner. Questions for flat-minima optimization of modern neural networks. *arXiv preprint arXiv:2202.00661*, 2, 2022.

Jing Yu Koh, Daniel Fried, and Ruslan Salakhutdinov. Generating images with multimodal language models. *arXiv preprint arXiv:2305.17216*, 2023a.

Jing Yu Koh, Ruslan Salakhutdinov, and Daniel Fried. Grounding language models to images for multimodal generation. *arXiv preprint arXiv:2301.13823*, 2023b.

Junnan Li, Dongxu Li, Silvio Savarese, and Steven Hoi. Blip-2: Bootstrapping language-image pre-training with frozen image encoders and large language models. *arXiv preprint arXiv:2301.12597*, 2023.

Xiang Lisa Li, Ari Holtzman, Daniel Fried, Percy Liang, Jason Eisner, Tatsunori Hashimoto, Luke Zettlemoyer, and Mike Lewis. Contrastive decoding: Open-ended text generation as optimization. *arXiv preprint arXiv:2210.15097*, 2022.

Tsung-Yi Lin, Michael Maire, Serge Belongie, James Hays, Pietro Perona, Deva Ramanan, Piotr Dollár, and C Lawrence Zitnick. Microsoft coco: Common objects in context. In *Computer Vision–ECCV 2014: 13th European Conference, Zurich, Switzerland, September 6-12, 2014, Proceedings, Part V 13*, pp. 740–755. Springer, 2014.

Haotian Liu, Chunyuan Li, Qingyang Wu, and Yong Jae Lee. Visual instruction tuning. *arXiv preprint arXiv:2304.08485*, 2023.

Michael S Matena and Colin A Raffel. Merging models with fisher-weighted averaging. *Advances in Neural Information Processing Systems*, 35:17703–17716, 2022.

Ron Mokady, Amir Hertz, and Amit H Bermano. Clipcap: Clip prefix for image captioning. *arXiv preprint arXiv:2111.09734*, 2021.

Igor Molybog, Peter Albert, Moya Chen, Zachary DeVito, David Esiobu, Naman Goyal, Punit Singh Koura, Sharan Narang, Andrew Poulton, Ruan Silva, et al. A theory on adam instability in large-scale machine learning. *arXiv preprint arXiv:2304.09871*, 2023.

Nasrin Mostafazadeh, Nathanael Chambers, Xiaodong He, Devi Parikh, Dhruv Batra, Lucy Vanderwende, Pushmeet Kohli, and James Allen. A corpus and evaluation framework for deeper understanding of commonsense stories. *arXiv preprint arXiv:1604.01696*, 2016.

Ivona Najdenkoska, Xiantong Zhen, and Marcel Worring. Meta learning to bridge vision and language models for multimodal few-shot learning. *arXiv preprint arXiv:2302.14794*, 2023.

Alexander Quinn Nichol, Prafulla Dhariwal, Aditya Ramesh, Pranav Shyam, Pamela Mishkin, Bob Mcgrew, Ilya Sutskever, and Mark Chen. Glide: Towards photorealistic image generation and editing with text-guided diffusion models. In *International Conference on Machine Learning*, pp. 16784–16804. PMLR, 2022.

Alec Radford, Jong Wook Kim, Chris Hallacy, Aditya Ramesh, Gabriel Goh, Sandhini Agarwal, Girish Sastry, Amanda Askell, Pamela Mishkin, Jack Clark, et al. Learning transferable visual models from natural language supervision. In *International conference on machine learning*, pp. 8748–8763. PMLR, 2021.

Colin Raffel, Noam Shazeer, Adam Roberts, Katherine Lee, Sharan Narang, Michael Matena, Yanqi Zhou, Wei Li, and Peter J Liu. Exploring the limits of transfer learning with a unified text-to-text transformer. *The Journal of Machine Learning Research*, 21(1):5485–5551, 2020.

Aditya Ramesh, Mikhail Pavlov, Gabriel Goh, Scott Gray, Chelsea Voss, Alec Radford, Mark Chen, and Ilya Sutskever. Zero-shot text-to-image generation. In *International Conference on Machine Learning*, pp. 8821–8831. PMLR, 2021.

Aditya Ramesh, Prafulla Dhariwal, Alex Nichol, Casey Chu, and Mark Chen. Hierarchical text-conditional image generation with clip latents. *arXiv e-prints*, pp. arXiv–2204, 2022.

Keisuke Sakaguchi, Ronan Le Bras, Chandra Bhagavatula, and Yejin Choi. Winogrande: An adversarial winograd schema challenge at scale. *Communications of the ACM*, 64(9):99–106, 2021.

Jascha Sohl-Dickstein, Eric Weiss, Niru Maheswaranathan, and Surya Ganguli. Deep unsupervised learning using nonequilibrium thermodynamics. In *International conference on machine learning*, pp. 2256–2265. PMLR, 2015.

Hugo Touvron, Thibaut Lavril, Gautier Izacard, Xavier Martinet, Marie-Anne Lachaux, Timothée Lacroix, Baptiste Rozière, Naman Goyal, Eric Hambro, Faisal Azhar, Aurelien Rodriguez, Armand Joulin, Edouard Grave, and Guillaume Lample. Llama: Open and efficient foundation language models, 2023.

Maria Tsimpoukelli, Jacob L Menick, Serkan Cabi, SM Eslami, Oriol Vinyals, and Felix Hill. Multimodal few-shot learning with frozen language models. *Advances in Neural Information Processing Systems*, 34:200–212, 2021.

Aaron Van Den Oord, Oriol Vinyals, et al. Neural discrete representation learning. *Advances in neural information processing systems*, 30, 2017.

Yizhong Wang, Yeganeh Kordi, Swaroop Mishra, Alisa Liu, Noah A Smith, Daniel Khashabi, and Hannaneh Hajishirzi. Self-instruct: Aligning language model with self generated instructions. *arXiv preprint arXiv:2212.10560*, 2022.

Jason Wei, Maarten Bosma, Vincent Zhao, Kelvin Guu, Adams Wei Yu, Brian Lester, Nan Du, Andrew M Dai, and Quoc V Le. Finetuned language models are zero-shot learners. In *International Conference on Learning Representations*, 2021.

Mitchell Wortsman, Gabriel Ilharco, Samir Ya Gadre, Rebecca Roelofs, Raphael Gontijo-Lopes, Ari S Morcos, Hongseok Namkoong, Ali Farhadi, Yair Carmon, Simon Kornblith, et al. Model soups: averaging weights of multiple fine-tuned models improves accuracy without increasing inference time. In *International Conference on Machine Learning*, pp. 23965–23998. PMLR, 2022.

Michihiro Yasunaga, Armen Aghajanyan, Weijia Shi, Rich James, Jure Leskovec, Percy Liang, Mike Lewis, Luke Zettlemoyer, and Wen-tau Yih. Retrieval-augmented multimodal language modeling. *arXiv preprint arXiv:2211.12561*, 2022.

Qinghao Ye, Haiyang Xu, Guohai Xu, Jiabo Ye, Ming Yan, Yiyang Zhou, Junyang Wang, Anwen Hu, Pengcheng Shi, Yaya Shi, et al. mplug-owl: Modularization empowers large language models with multimodality. *arXiv preprint arXiv:2304.14178*, 2023.

Jiahui Yu, Yuanzhong Xu, Jing Yu Koh, Thang Luong, Gunjan Baid, Zirui Wang, Vijay Vasudevan, Alexander Ku, Yinfei Yang, Burcu Karagol Ayan, et al. Scaling autoregressive models for content-rich text-to-image generation. *Transactions on Machine Learning Research*, 2022.

Lili Yu, Bernie Huang, Candace Ross, Vladimir Karpukhin, Hu Xu, Naman Goyal, Dmytro Okhonko, Mandar Joshi, Gargi Ghosh, Mike Lewis, et al. Scaling autoregressive multi-modal models: Pre-training and instruction tuning. *arXiv preprint arXiv:2201.07520*, 2023.

Susan Zhang, Stephen Roller, Naman Goyal, Mikel Artetxe, Moya Chen, Shuohui Chen, Christopher Dewan, Mona Diab, Xian Li, Xi Victoria Lin, et al. Opt: Open pre-trained transformer language models. *arXiv preprint arXiv:2205.01068*, 2022.

Chunting Zhou, Pengfei Liu, Puxin Xu, Srini Iyer, Jiao Sun, Yuning Mao, Xuezhe Ma, Avia Efrat, Ping Yu, Lili Yu, et al. Lima: Less is more for alignment. *arXiv preprint arXiv:2305.11206*, 2023.

Deyao Zhu, Jun Chen, Xiaoqian Shen, Xiang Li, and Mohamed Elhoseiny. Minigpt-4: Enhancing vision-language understanding with advanced large language models. *arXiv preprint arXiv:2304.10592*, 2023.